Accepted Manuscript

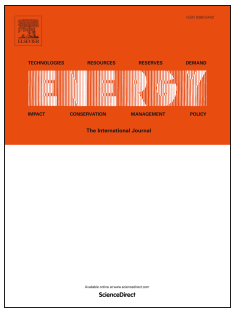

Selective low temperature chemical looping combustion of higher alkanes with Cu- and Mn- oxides

Fatih Güleç, Will Meredith, Cheng-Gong Sun, Colin E. Snape

PII: S0360-5442(19)30298-1

DOI: https://doi.org/10.1016/j.energy.2019.02.099

Reference: EGY 14741

To appear in: *Energy*

Received Date: 22 November 2018

Revised Date: 12 February 2019

Accepted Date: 13 February 2019

Please cite this article as: Güleç F, Meredith W, Sun C-G, Snape CE, Selective low temperature chemical looping combustion of higher alkanes with Cu- and Mn- oxides, *Energy* (2019), doi: https://doi.org/10.1016/j.energy.2019.02.099.

Selective Low Temperature Chemical Looping Combustion of Higher Alkanes with Cu- and Mn-Oxides

Fatih Güleç*, Will Meredith, Cheng-Gong Sun, and Colin E. Snape

University of Nottingham, Faculty of Engineering, Energy Technologies Building, Triumph Road, Nottingham NG7 2TU, UK

*Corresponding author: Fatih.Gulec@nottingham.ac.uk

Abstract

Chemical looping combustion (CLC) of n-hexadecane and n-heptane with copper and manganese oxides (CuO and Mn_2O_3) has been investigated in a fixed bed reactor to reveal the extent to which low temperature CLC can potentially be applicable to hydrocarbons. The effects of fuel to oxygen carrier ratio, fuel feed flow rate, and fuel residence time on the extent of combustion are reported. Methane did not combust, while near complete conversion was achieved for both n-hexadecane and n-heptane with excess oxygen carrier for CuO. For Mn_2O_3, complete reduction to Mn_3O_4 occurred, but the extent of combustion was controlled by the much slower reduction to MnO. Although the extent of cracking is relatively small in the absence of cracking catalysts, for the mechanism to be selective for higher hydrocarbons suggests that the reaction with oxygen involves radicals or carbocations arising from bond scission. Sintering of pure CuO occurred after repeated cycles, but this can easily be avoided using a support, such as alumina. The fact that higher hydrocarbons can be combusted selectively at 500 °C and below, offers the possibility of using CLC to remove these hydrocarbons and potentially other organics from hot gas streams.

Keywords: CO_2 capture, Chemical Looping Combustion (CLC), Liquid fuels, Copper-based oxygen carrier, Manganese-based oxygen carrier

1. Introduction

Chemical looping combustion (CLC) is an emerging approach for CO_2 capture where metal oxides are used as the oxygen source in place of air to combust the fuel [1-6]. This can potentially result in considerable energy savings compared to the more established technologies of post-combustion, pre-combustion and oxy-combustion [7-12]. In contrast to these technologies, CLC does not require a CO_2 separation stage nor an air separation unit [13]. Therefore, energy and cost penalties, due to gas separation operations, can be avoided by the application of CLC [14, 15].

There has been considerable research on the use of CLC for both gas and solid fuel combustion as summarised in reviews by Lyngfelt et al. [16], Matisson et al. [17] and Adanez et al. [18, 19], but there are fewer studies on liquid fuels. Cao et al. [20] investigated the gasification of bitumen and asphalt in an upstream process, with the synthesis gases combusted over a lanthanum promoted copper-based oxygen carrier in a laboratory scale batch fluidised bed reactor. Hoteit et al. [13] carried out CLC experiments with n-dodecane over a nickel-based oxygen carrier, $NiAl_{0.44}O_{1.67}$, at 800 and 900 °C in a batch fluidised bed reactor. They found the complete combustion of n-dodecane to CO_2 and H_2O if the residence time was long enough in the batch fluidised bed used. Bao et al. [21] conducted combustion experiments using n-heptane in a saturated nitrogen flow as the fuel and an Fe based oxygen carrier in a laboratory scale fluidised bed reactor. Both Cao et al. [20] and Hoteit et al. [13] agreed that at the end of the reduction step, there was no carbon deposition on Ni- and Cu-based oxygen carriers unlike with Fe_2O_3 [21]. Serrano et al. [22] reported on the combustion of diesel, mineral and synthetic lubricant oils with Fe based oxygen carriers at different oxygen carrier to fuel ratios, and demonstrated that it was possible to reach higher than 90 % combustion efficiency when using an oxygen carrier to fuel ratio of greater than 3 at 900 °C.

Moldenhauer et al. [23-27] reported the combustion of kerosene, fuel oil, and vacuum residue with the oxygen carriers; Ni-, Mn-, and Cu- based zirconium oxide, ilmenite, and calcium manganite in a 300 W circulating fluidised bed reactor at the temperatures of 750-900 °C. Very high fuel conversions to CO_2 were achieved, > 95 % for NiO and CuO based oxygen carriers [24], and over 83% for Mn_3O_4 [23]. They also demonstrated that it was possible to achieve CO_2 yields of above 99 % with ilmenite at 950 °C [26]. Moldenhauer et al. [24] also suggested that although fuel conversion at the lowest temperatures (650-700 °C) was still relatively high, the CLOU properties, where the oxygen carriers can release their oxygen can be neglected at such temperatures [28]. CLOU requires temperatures of >800 °C for CuO to reduce to Cu_2O, >700 °C for Mn_2O_3 to reduce to Mn_3O_4 and >750 °C for Co_3O_4 to reduce CoO [17]. Although CuO decomposition is not thermodynamically favourable

below 700 °C according to the positive Gibbs free energy values, the reaction between CuO and C can be favourable between 200-1000 °C as described by Siriwardane et al [29]. Additionally, a two stage CLC process, that is a combination of normal CLC with low temperature CLC, has been suggested to improve the CO_2 purity in the fuel combustion gases by Xu et al. [30]. The cement supported Cu-based oxygen carrier demonstrated relatively fast oxidation and reduction rates with air and carbon monoxide respectively, at temperatures as low as 300 °C in TGA [30]. Gas-solid kinetics of an active Ni-based oxygen carrier have been investigated with H_2 and CO (mixed with CO_2), and CH_4 (mixed with steam) as reducing agents at temperatures between 500 °C and 800 °C by Medrano et al. [31]. While the fully oxidised Ni-based carrier did not show activity at low temperatures, the oxygen carrier containing some remaining reduced Ni demonstrated reduction with CH_4 (mixed with steam) [31].

Oil refineries account for approximately 4 % of the global CO_2 emissions and Fluid Catalytic Cracking (FCC) units are responsible for roughly a quarter of these [10, 22, 32], and so it was considered that CO_2 capture via CLC could potentially be applied to FCC. Combustion to remove coke in the regenerator proceeds at *ca*. 700 °C in the air and, for CLC, this can be accomplished by adding oxygen carriers to FCC catalysts. The oxygen carrier would need to be effectively inert with respect to cracking at temperatures close to 500 °C. However, in tests using the standard microactivity reactor (MAT) for FCC [33], CLC of n-hexadecane occurred with CuO mechanically mixed with an FCC catalyst. The preliminary cracking results of n-hexadecane over FCC catalyst and CuO mixed FCC catalyst are presented in Table A1 (Appendix A). This observation provided the motivation to investigate the applicability of low temperature CLC as a process for removing organic contaminants from hot gas streams.

In this study, CLC of n-hexadecane and n-heptane was investigated over two different oxygen carriers, CuO and Mn_2O_3, in a fixed bed MAT reactor at the relatively low temperature of 482 °C. Control experiments were conducted with methane over CuO at the same temperature. The effects of (i) fuel to oxygen carrier equivalence ratio, (ii) fuel residence time into the reactor, (iii) the reactor temperature, and (iv) multiple cycles of CuO and CuO/Al_2O_3 on the extent of CLC have been investigated. This study is the first report on how CLC can selectively be applied to higher hydrocarbons and potentially other organic compounds in methane and other gas streams.

2. Materials and methods

2.1. Liquid fuels and oxygen carriers

n-Hexadecane ($C_{16}H_{34}$, purity: 99 %) and n-heptane (C_7H_{16}, purity: 99 %) were purchased from Alfa Aesar and Prolabo Chemicals, respectively. The two oxygen carriers, namely, CuO (purity: 99 %) and Mn_2O_3 (purity: 99 %), were purchased from Sigma Aldrich. A mixture of 20 % CH_4 and 80 % He was used to investigate the combustion of methane under the conditions used.

To investigate the effect of using supported oxygen carriers on the low temperature CLC, CuO/Al_2O_3 having a mass ratio of 80:20 was prepared using co-precipitation method reported by Chuang et al. [34-36]. Approximately 80 ml of $Cu(NO_3)_2$ (1.26 M) solution was mixed with about 94 ml of $Al(NO_3)_3$ (0.42 M) solution at 500 rpm for 2 min on a magnetic stripper. The quantities of nitrate solutions used were adjusted according to the final mass ratio of $CuO:Al_2O_3$ as to be 80:20. Secondly, an approximately 30 % excess volume of Na_2CO_3 (46 ml, 2.83 M) was added into the nitrate solutions. The resulting mixture was agitated at 750 rpm for 2 min using a magnetic stirrer. The resulting precipitate was then centrifuged at 20 rpm for 4 min, and the slurry was then washed with deionised water using a ratio about 15:1 (water:precipitate). The centrifuging and washing processes were repeated five times until all of the sodium ions were removed from the slurry. The slurry was then dried at 120 °C for 12 h and sieved into the size range of 53-300 μm. Finally, the dried precipitate was calcined in a tubular furnace at 950 °C for 2h.

The fresh and used oxygen carriers were characterised to evaluate the effects of CLC combustion on their structure. The surface morphologies and particle size distributions were investigated by electron microscopy using a Philips XL30 FEI SEM instrument. Skeletal densities were defined using a Micromeritics AccuPyc II 1340 Gas Pycnometer. The crystalline phase of the samples was analysed using a Simens D500 diffractometer, with the samples scanned over a 2θ range of 20° to 80°, with a 2θ step size of 0.05° and a step time of 2 s. Furthermore, the percentage distribution of the reduced CuO and Mn_2O_3 states were estimated by comparing the integrated intensities of the diffraction peaks from each of the known phases.

2.2. Baseline experiments

2.2.1. Thermal cracking of n-hexadecane and n-heptane

Thermal cracking of the liquid hydrocarbons was carried out in a MAT fixed-bed reactor illustrated in Fig. 1 [33]. Although a fluidised bed reactor is the most common reactor type used for CLC tests, such experiments have also been conducted in fixed-bed reactors [3, 5, 37, 38]. The experimental

unit comprised a Pyrex glass cylindrical reactor with an internal diameter of 15 mm and a length of 270 mm, a temperature controlled tubular furnace, a syringe pump, a liquid product receiver and a gas bag. Firstly, a small amount of glass wool was placed inside the glass reactor, which was then located in the tubular furnace. The reactor temperature set to 482 °C since the potential of low temperature CLC of higher hydrocarbons became apparent during the cracking of n-hexadecane over oxygen carriers containing FCC catalysts at 482 °C while investigating whether CLC could be integrated with FCC for CO_2 capture. When this temperature was attained, the reactor was purged with N_2 for 10 min with a flow of 20 ml/min. Except where stated otherwise, approximately 0.60 ml of the hydrocarbon fuel, either n-hexadecane or n-heptane, was then introduced to the reactor at a rate of 0.03 ml/min for 20 min. During this injection period, the N_2 flow was set to 1 ml/min and the fuel injection temperature was controlled by a vertically located thermocouple in contact with the glass wool bed. After injection, the reactor and product recovery system were purged with a N_2 flow of 20 ml/min for 15 min.

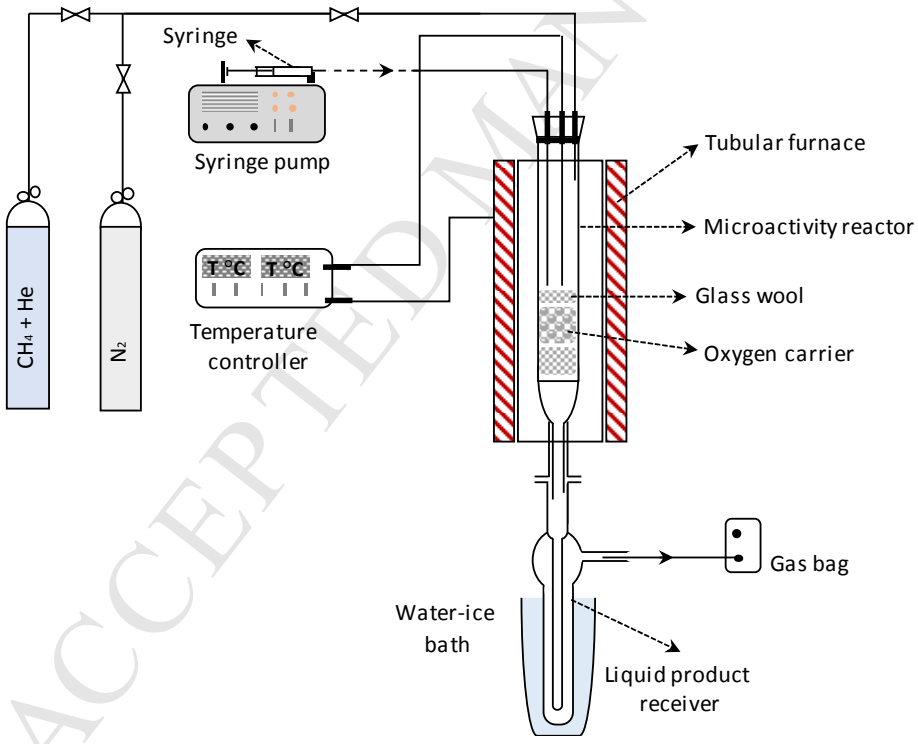

Fig. 1. The fixed bed microactivity reactor system (MAT), (modified from ASTM D3907-13) [33].

The receiver, placed within a water-ice bath condensed the liquid products, and the gases were collected in a 1 L gas bag. The liquid products were analysed using a Clarus 580 GC (Perkin Elmer Elite-1 phase 60 m x 0.25 mm x 0.25 µm capillary column) fitted with a FID detector. An aliquot, 1 µl

of the liquid sample (diluted in dichloromethane) was injected at 250 °C with helium as the carrier gas. The gas products collected in a gas bag were immediately analysed using a Clarus 580 GC fitted with FID and TCD detectors for the hydrocarbon and non-hydrocarbon gases respectively, operating at 200 °C. 5 ml of gas samples were injected (split ratio 10:1) at 250 °C with separation performed on an alumina plot fused silica 30 m x 0.32 mm x 10 µm column, with helium as the carrier gas. The oven temperature was programmed from 60 °C (13 min hold) to 160 °C (10 min hold) at 10 °C/min.

2.2.2. The combustion of methane over CuO at low temperature

The CLC of methane (in the form of a gas mixture: 20 % CH_4 + 80 % He) was investigated with CuO under similar experimental conditions using the same reactor set-up. The stoichiometric amount of methane (approximately 210 ml methane) was introduced to 3 g of CuO placed in the microactivity reactor (MAT) with a flow rate 20 ml/min for the 20 % CH_4/80 % He mixture at 482 °C. During this injection, the N_2 flow was switched off. After injection, the reactor and product recovery system were purged with a N_2 flow of 20 ml/min for 15 min, and the products collected in the gas bag were immediately analysed by using the Clarus 580 GC fitted with FID and TCD detectors.

2.3. CLC of liquid fuels

The CLC tests of n-hexadecane and n-heptane with oxygen carriers were conducted in the same experimental set-up, using the same heating, N_2 flow and sample injection protocols as for the thermal cracking baseline tests. The oxygen carriers; 3 g CuO or 6 g Mn_2O_3, with masses selected to give the same oxygen transfer capacity, were placed between two pieces of glass wool in the glass reactor. In addition to the liquid and gaseous products analysed as described above by GC, the coke deposited on the used oxygen carriers was quantified by elemental analysis using a LECO 628 CHN instrument.

2.3.1. The effects of fuel to oxygen carrier equivalence ratio

The equivalence ratio is the ratio of molar flow rate of fuel to that of oxygen, ϕ, [39, 40]. The definition of the equivalence ratio is asymmetrical relative to fuel-lean ($0<\phi<1$) and fuel-rich ($1<\phi<\infty$) conditions [40]. To demonstrate the effects of fuel to oxygen carrier equivalence ratio, the liquid fuels were introduced to the fixed-bed reactor at 0.03 ml/min for different fuel to oxygen carrier equivalence ratios (ϕ: 0.7, 1.0, 1.3, and 2.0), with all other experimental conditions unchanged. For the different equivalence ratios, while the amount of oxygen carriers were kept same, 3 g of CuO and 6 g of Mn_2O_3, the amount of fuel injected was varied (n-hexadecane 0.158, 0.226, 0.293, and 0.452 mL; n-heptane 0.175, 0.251, 0.321, and 0.502 mL).

2.3.2. The effects of fuel feed rate and residence time

To investigate the effects of fuel residence time within the reactor, the combustion of n-hexadecane was carried out using 2 g of inert sand mixed with the 3 g of CuO (Sand:CuO; 40:60 wt. %) at different volumetric feed flow rates; 0.03, 0.1, 0.2, 1.4 ml/min for ϕ: 0.7. This has the effect of increasing the volume of the reactor bed by 70 %, and so increasing the residence time that the liquid feed was in contact with the oxygen carrier by the same amount. In addition to the increase in bed volume, the residence time of n-hexadecane in the reactor was also investigated using different carrier gas volumetric flow rates of 0.5, 1.0, and 2.0 ml/min over CuO at 0.2 ml/min feed flow rate for ϕ being 0.7.

2.3.3. The effects of temperature

The CLC of n-hexadecane was investigated with CuO using a fuel to oxygen carrier equivalence ratio of 0.7 with a feed flow rate of 0.2 ml/min at eight different temperatures of 320, 360, 380, 400, 440, 482, 520, 560 °C. The heating rate, N_2 flow, sample injection and product collection protocols were the same as for the thermal cracking baseline tests.

2.3.4. Multiple cycle tests of CuO with n-hexadecane combustion

The impact of repeated cycles of n-hexadecane combustion on the performance of the oxygen carriers was investigated with bulk CuO and a fuel to oxygen carrier equivalence ratio of 1.3 at a feed flow rate of 0.03 ml/min over seven reduction and oxidation cycles. For the first five cycles, after each reduction of CuO with n-hexadecane, the reduced form Cu particles were oxidised at 700 °C for 20 min in a muffle furnace and then reused for the next combustion experiment. To ensure complete oxidation of the reduced form oxygen carrier for the 6^{th} and 7^{th} cycles it was re-oxidised at 700 °C and 900 °C for 60 min respectively. The multiple cycle tests were repeated using CuO/Al_2O_3 (80:20 wt. %), which was prepared by the co-precipitation method presented by Chuang et al. [34-36]. For the seven cycles, after each reduction of CuO/Al_2O_3 with n-hexadecane, the reduced form Cu particles were re-oxidised at 700 °C for 20 min and then reused for the next cycle of combustion.

2.3.5. Characterisation of fresh and used oxygen carriers

To characterise the oxygen carriers (CuO, CuO/Al_2O_3, and Mn_2O_3), the true density of both the fresh and used carriers were measured by a Micromeritics AccuPyc II 1340 Gas Pycnometer. The particle size distributions of oxygen carriers were measured by sieving, ranging from 53 to 300 µm. The fragmentation and agglomeration of fresh and used CuO and CuO/Al_2O_3 were imaged by Scanning

Electron Microscopy (SEM) using a JEOL JSM 6490LV microscope operated at 20 kV accelerated voltage using secondary electron imaging (SEI) modes. The crystalline phases of the oxygen carriers were measured by a Siemens D500 X-ray powder diffractometer (XRD) with Cu-Kα having a wavelength of 0.15406 nm radiation operating at 40 kV and 35 mA. The samples were scanned over a 2θ range of 20° to 80° with a step size of 0.02° and a step time of 2 s. The XRD results were correlated with the references, Joint Committee on Powder Diffraction Standards (JCPDS).

2.4. Data evaluation

The equivalence ratio, ϕ, was calculated using Eq. 1 which was modified from [39, 40]. The combustion ratio % is defined as the ratio of the actual amount of CO_2 produced by the combustion to the maximum amount that can be obtained for both fuel-lean and fuel-rich conditions, and it was calculated using Eq. 2.

$$\phi = \frac{b.n_F}{n_{OC}} \quad (1)$$

ϕ: Equivalence ratio of fuel to oxygen carrier.

n_{OC}, n_F : Mol of oxygen carrier and liquid fuel, respectively.

b : Stoichiometric coefficient for each reaction.

$$Combustion\,(wt.)\,\% = \frac{w_{CO_2}}{w_{CO_{2,\max}}} * 100 \quad (2)$$

w_{CO_2} : Actual weight of CO_2 after combustion of liquid fuel with oxygen carrier.

$w_{CO_2,max}$: Maximum weight of CO_2 that can be produced either full combustion of liquid fuel (fuel-lean experiments, $0<\phi<1$) or fully reduction of oxygen carrier (fuel-rich experiments, $1<\phi<\infty$).

3. Results and discussion

3.1. Baseline experiments

Minimal cracking of the feeds occurred without oxygen carriers present in the reactor, with only 5 wt. % of n-hexadecane found to be converted to C_1-C_6 gases (Table 1). n-Heptane was even less reactive with only 2 wt. % of gases obtained.

Table 1. Thermal cracking results for n-hexadecane and n-heptane

Fuel	Cracked products (C_{1-5}, wt. %)
n-hexadecane ($C_{16}H_{34}$)	5.0 ±0.4
n-heptane (C_7H_{16})	2.0 ±0.1

To ascertain the extent of methane CLC at 482 °C, a stoichiometric quantity of methane was tested with CuO. This resulted in minimal combustion of methane, with the resultant products composed of only 0.9 wt. % CO_2 and over 99 wt. % unconverted methane (Table 2). This finding was expected from literature reports of methane CLC using CuO occurring at around 800 °C [41-44].

Table 2. Combustion products from methane with CuO at 482 °C

Fuel	CO_2 (%)	CH_4 (%)
Methane (CH_4)	0.9 ±0.004	99.1 ±0.004

3.2. The effects of fuel to oxygen carrier equivalence ratio (ϕ)

The extents of CLC for-hexadecane and n-heptane with CuO and Mn_2O_3 were calculated using Eq. 2, and are presented in Fig. 2 with respect to the different equivalence ratios of fuel to the oxygen carriers, which were calculated on the basis of the reduction of CuO to Cu and Mn_2O_3 to MnO.

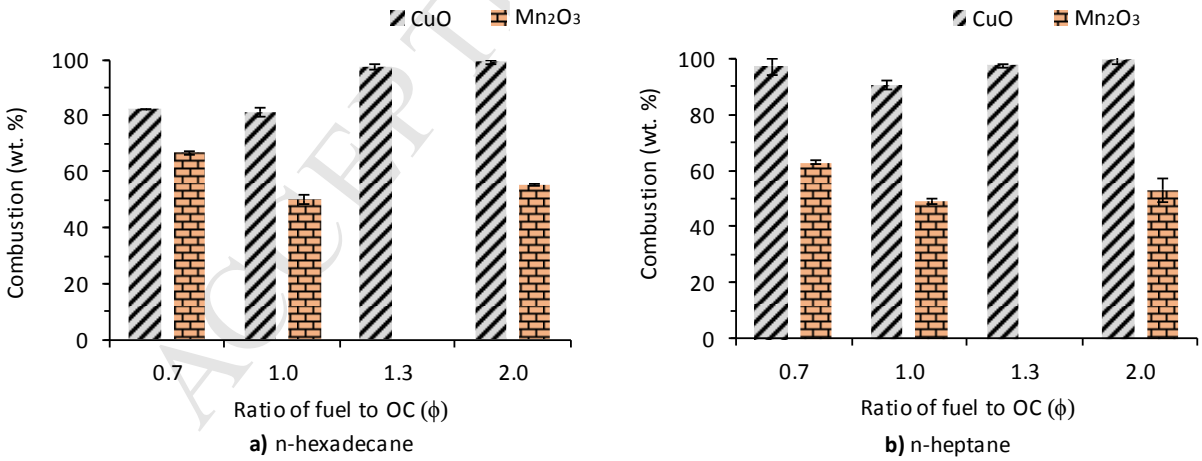

Fig. 2. Combustion % of a) n-hexadecane; b) n-heptane over CuO and Mn_2O_3 for different fuel to oxygen carrier equivalence ratios (ϕ: 0.7, 1.0, 1.3, and 2.0) for 0.03 ml/min feed flow rate at 482 °C (the error bars represents the standard deviation calculated by triple experiments).

Fig. 2 shows that it is possible to achieve almost complete combustion for both n-hexadecane and n-heptane using CuO as an oxygen carrier in fuel rich conditions at $\phi \geq 1.3$. However, when the fuel/CuO equivalence ratio is stoichiometric at 1.0, the extent of combustion fell to 80 wt. % for n-hexadecane and 90 wt. % for n-heptane. This can be explained by the uneven dispersion of the liquid fuels across the oxygen carrier bed. Following the tests, material on one side of the bed was observed to still be black in colour, along its whole length, indicating the presence of CuO, while the rest of the bed was red, having clearly been reduced to Cu. This proves that some of the fuel may pass through mainly the reduced part of the oxygen carrier bed instead of the part having oxidised oxygen carriers and consequently the theoretical extent of combustion is not attained. When the fuel to oxygen carrier equivalence ratio was decreased to 0.7 to give fuel lean conditions, the extent of combustion increased from 90 to 97 wt. % for n-heptane, but remained at close to 80 wt. % for n-hexadecane.

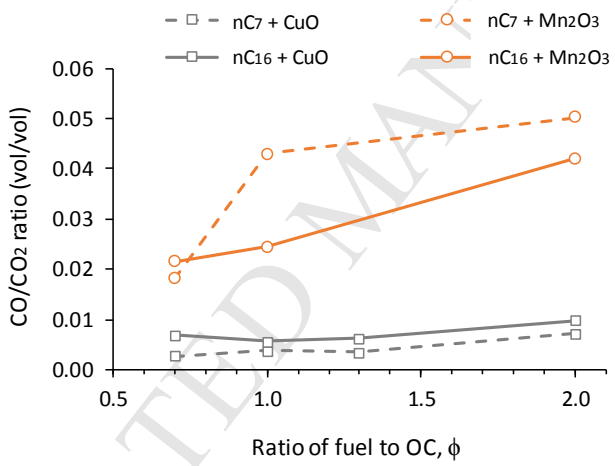

Fig. 3. The volumetric ratio of CO/CO_2 for n–hexadecane and n-heptane combustion with CuO and Mn_2O_3 for 0.03 ml/min fuel feed flow rate at ϕ: 0.7, 1.0, 1.3, and 2.0 fuel to oxygen carrier equivalence ratios, 482 °C.

For Mn_2O_3, the extent of combustion fell from 56 to 50 wt. % as the equivalence ratio was decreased from 2.0 to 1.0 for both alkanes (Fig.2). Moving to fuel-lean conditions with an equivalence ratio of 0.7, the extent of combustion increased to 67 wt. % for n-hexadecane and 63 wt. % for n-heptane. The lower extent of combustion apparent with Mn_2O_3 can be attributed to the sequential reduction step of the oxygen carrier, $Mn_2O_3 \rightarrow Mn_3O_4 \rightarrow MnO$. Approximately one-third of the required oxygen comes from the first reduction step ($Mn_2O_3 \rightarrow Mn_3O_4$). The XRD results (Section 3.7) show that, while the Mn_2O_3 was almost fully reduced, the recovered samples were composed of mixtures of Mn_3O_4

and MnO. Therefore, the lower combustion efficiencies compared to CuO arise from the slow second reduction step (Mn_3O_4→MnO). Furthermore, due to the similarity of the combustion at the equivalence ratio of 1.0-2.0, the combustion at the equivalence ratio of 1.3 was not investigated.

The low volumetric ratios of CO to CO_2 obtained from CLC are presented in Fig. 3. However, the ratios are higher with Mn_2O_3 (<0.05) compared than for CuO (<0.01). Previous studies at higher temperatures have also observed low proportions of CO for diesel [10], kerosene [23], synthetic oil [10, 22], and asphalt-fuelled [45] combustion with oxygen carriers.

3.3. Liquid fuel feed rate and residence time

These were investigated using n-hexadecane with CuO and sand mixtures (SaCuO) at different volumetric feed and carrier gas (N_2) flow rates. The extent of combustion was calculated with using Eq. 2, and the results are given in Fig. 4 with respect to the volumetric feed flow rates (Fig. 4a) and carrier gas flow rates (Fig. 4b).

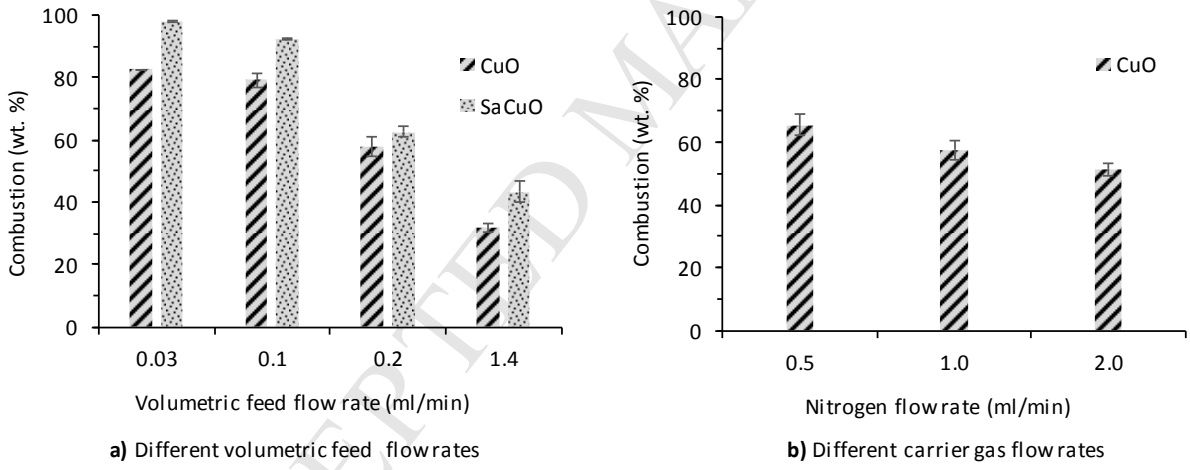

Fig. 4. Combustion % of n-hexadecane over CuO and SaCuO a) at different volumetric feed flow rates (0.03, 0.1, 0.2, and 1.4 ml/min) for ϕ: 0.7 at 482 °C; b) Combustion % of n-hexadecane over CuO for ϕ: 0.7 at 0.2 ml/min, 482 °C using different carrier gas flow rates (0.5, 1.0, 2.0 ml/min).

As seen in Fig. 4a**,** the extent of combustion was 80 and 99 wt. % with and without sand mixed CuO (SaCuO) at the lowest feed rate of 0.03 ml/min. Blending with sand increased the residence time and so dispersion of the liquid fuel within the oxygen carrier bed. The calculated vapour residence time of 13.1 s with a feed flow rate of 0.03 ml/min was increased to 20.6 s by the dilution of the CuO in the sand. The same trend can be seen for the other volumetric flow rates. Increasing the feed rate

from 0.03 ml/min gave lower conversions due to the residence time decreasing, but the effect was relatively minor until feed rates were higher than 0.1 ml/min. At higher rates, the decrease was greater, reflecting the decrease in residence time from 5.0 to 0.4 s with an increase in volumetric feed flow rate from 0.1 to 1.4 ml/min. A decrease in conversion was also brought about by increasing the carrier gas flow rate from 0.5 to 2 ml/min (Fig. 4b). The relatively minor extent of this decrease is evidence that the injected n-hexadecane was completely vaporised, as in the vapour phase, increasing the carrier gas flow by this extent would only have increased the residence time from 2.5 to 2.8 s.

3.4. The effect of temperature

Fig. 5 illustrates that the combustion of n-hexadecane with CuO fell from 80 to 40 % as the temperature decreased from 560 to 380 °C, although the residence time increased from 2.4 to 3.0 s due to the temperature decreasing. The extent of combustion was negligible at 360 °C with a residence time of 3.2 s. Additional discussion about the dramatic decrease below 380 °C are presented in the Section 3.8.

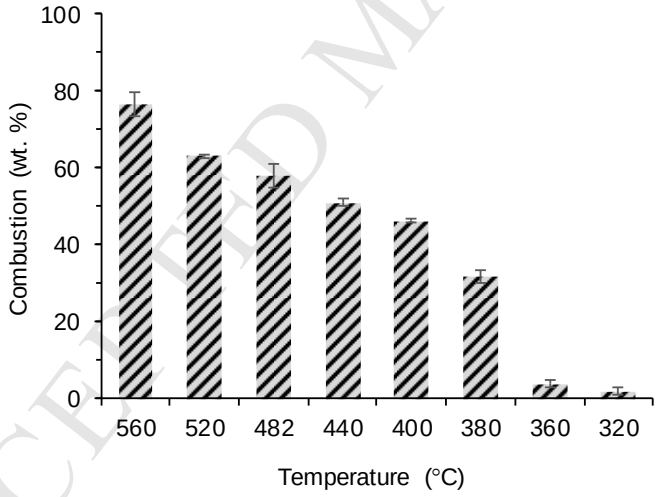

Fig. 5. Combustion % of n-hexadecane over CuO for ϕ: 0.7 at 0.2 ml/min at eight different temperatures from 320 to 560 °C.

3.5. Multiple cycles of n-hexadecane combustion with CuO

The results for the seven multi-cycle tests for n-hexadecane combustion at 482 °C, with re-oxidation after each step, both bulk oxygen carrier (CuO) and supported oxygen carrier (Al_2O_3) are shown in Fig. 6. It was possible to achieve full combustion, clearly with complete reduction and re-oxidation being achieved for both bulk CuO and CuO/Al_2O_3 for the first three cycles. However, for bulk CuO,

following the 4th and 5th cycles only 85 wt. % combustion occurred, probably due to the onset of sintering of the oxygen carrier, as shown in Fig. B2 (Appendix B). The extent of combustion reduced further to 78 wt. % after the 6th cycle as the extent of sintering increased. Even after increasing the oxidation temperature to 900 °C in the 7th cycle, only a small increase in combustion to 81 wt. % was observed, indicating that it was impossible to completely re-oxidise the oxygen carrier regardless of the temperature used. It is well-established that such sintering may be addressed using supports with suitable impregnation or co-precipitation preparation methods [41, 46, 47]. As seen in Fig. 6, a combustion efficiency of about 99 wt. % was achieved for all seven cycles once an Al_2O_3 supported CuO oxygen carrier was used in the combustion reaction instead of bulk CuO. These results were confirmed by measuring the CO_2 evolved during the seven multiple cycles of combustion via mass spectroscopy (ThermoStar TM GSD 301T), as presented in Fig. B1 in Appendix B.

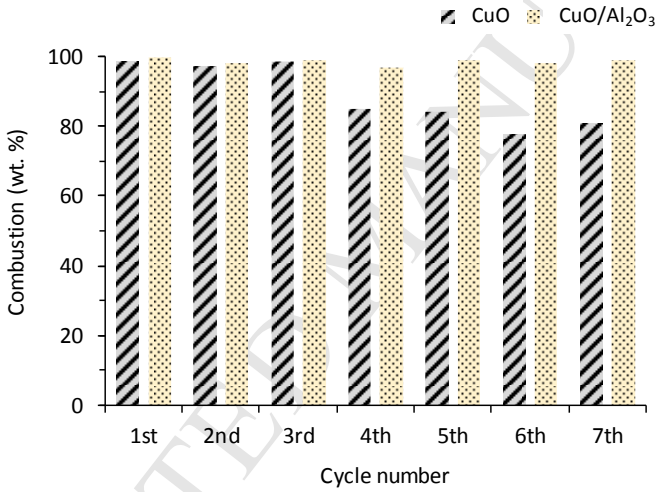

Fig. 6. Combustion % of n-hexadecane over CuO and CuO/Al_2O_3 for ϕ: 1.3 at 0.03 ml/min at 482 °C for seven cycles.

3.6. Characterisation of fresh and used oxygen carriers

The density and particle size distributions of the oxygen carriers before and after combustion are presented in Table 3. The density of reduced form CuO is very close to the density of metallic Cu (8.9 g/cm^3). Moreover, the density of reduced form Mn_2O_3 is between those for Mn_3O_4 (4.86 g/cm^3) and MnO (5.37 g/cm^3), indicating a mixture of Mn_3O_4 and MnO is present.

Elemental analysis confirmed that no carbon deposition had occurred on the oxygen carriers. The XRD patterns of fresh and used CuO (JCPDS no: 01-080-0076) and Mn_2O_3 (JCPDS no: 01-071-0636)

are presented in Fig. 7a and b, respectively. Fig. 7a-2 confirms the high proportion of reduced Cu after CLC of n-hexadecane. Further, the characteristic Cu peaks (JCPDS no: 01-085-1326) seen in Fig. 7a-3 demonstrate that full reduction from CuO to Cu occurred with a fuel to oxygen carrier equivalence ratio, ϕ, of 2.0 at 482 °C. The reduction from CuO with higher hydrocarbons to Cu may be attributed to the minimal external mass transfer at the low combustion temperatures. Chuang et al. [35, 36] have described that the reduction of CuO with either CO or H_2 followed the shrinking core mechanism, and proceeded via the intermediate, Cu_2O at higher temperatures when external mass transfer controlled the rate. However, at lower temperatures, the external mass transfer is minimal and CuO can reduce directly to Cu.

Table 3. The main characteristics of the oxygen carriers before and after combustion tests.

Properties	Before combustion			After combustion		
	CuO	CuO/Al_2O_3	Mn_2O_3	CuO*	CuO/Al_2O_3**	Mn_2O_3***
Density (g/cm^3)	6.22	5.79	4.84	8.63	7.51	4.99
Particle size (%)						
<53 µm	-	-	-	6.1	76.9	5.9
53-150 µm	100	100	100	13.4	23.1	51.1
151-300 µm	-	-	-	80.5	-	43.0

* Re-oxidised CuO after seven cycles. ** Re-oxidised CuO/Al_2O_3 after seven cycles. *** Re-oxidised Mn_2O_3 after one cycle.

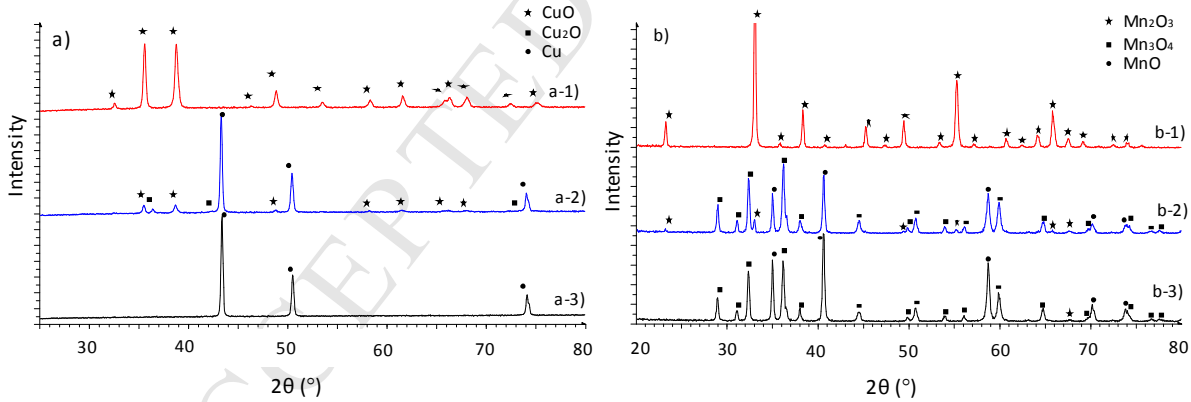

Fig. 7. Wide-angle XRD patterns of a) CuO; b) Mn_2O_3 before and after n-hexadecane combustion experiments; a-1) fresh CuO, a-2) used CuO at ϕ: 1.0, a-3) used CuO at ϕ: 2.0, b-1) fresh Mn_2O_3, b-2) used Mn_2O_3 at ϕ: 1.0, b-3) used Mn_2O_3 at ϕ: 2.0 for 0.03 ml/min n-hexadecane feed flow rate at 482 °C.

The XRD patterns of the Mn_2O_3 oxygen carrier used in the combustion of n-hexadecane for ϕ: 1.0 and 2.0 at 482 °C, shown in Fig. 7b-2 and 3, consist of mainly Mn_3O_4 and MnO (JCPDS no: 01-078-0424) in different ratios. These findings prove the sequential reduction steps of

$Mn_2O_3 \rightarrow Mn_3O_4 \rightarrow MnO$ under the combustion of higher hydrocarbons at low temperatures. The percentage distribution of the reduced Mn states is presented in Table 4. As already described, the first reduction step ($Mn_2O_3 \rightarrow Mn_3O_4$) is much faster than the second one ($Mn_3O_4 \rightarrow MnO$).

Table 4. XRD results of the fresh and used Mn_2O_3 in CLC for n-hexadecane at ϕ: 1.0 and 2.0 at 482 °C.

Sample	Mn_2O_3 (wt. %)	Mn_3O_4 (wt. %)	MnO (Wt. %)
Fresh Mn_2O_3	100	-	-
Used Mn_2O_3 at ϕ: 1.0	1	77	22
Used Mn_2O_3 at ϕ: 2.0	-	70	31

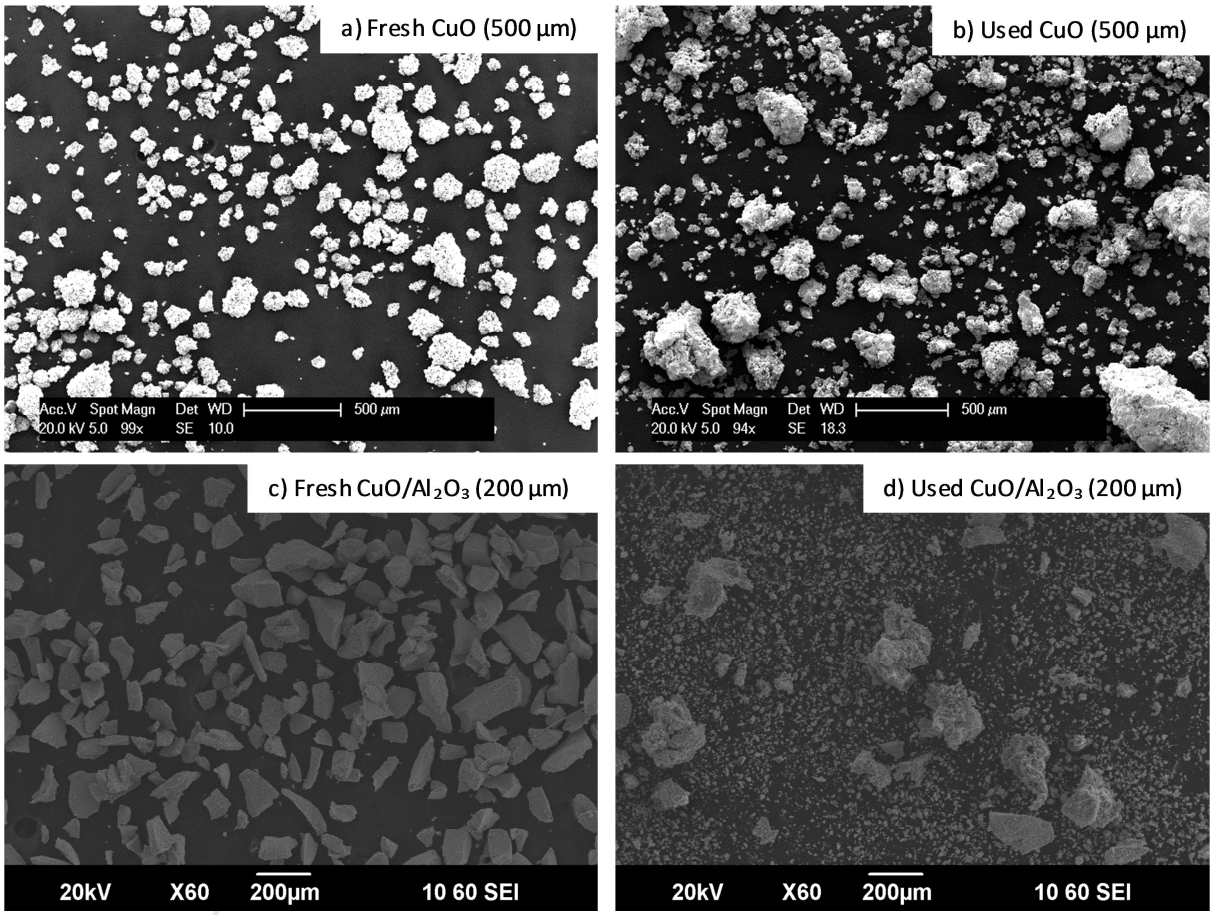

Fig. 8. SEM images of fresh CuO (a), CuO/Al_2O_3 (c) and used CuO (b), CuO/Al_2O_3 (d) after 7 cycles at ϕ: 1.3 (7 cycles) under a 0.03 ml/min n-hexadecane feed flow rate at 482 °C.

The particle size distributions measured by sieving and SEM for the fresh and used CuO and CuO/Al_2O_3 were compared after the 7 cycle test. SEM. (Fig. 8) indicates that the particle size of bulk CuO has increased due to sintering of the reduced Cu. Sieving indicated 81 wt. % of the particles were in the 150-300 µm range, with just 13 wt. % remaining in the initial size range of 53-150 µm

and 6 wt. % reduced in size to <53 μm (Table 3). On the other hand, using supported Cu, both sintering and agglomeration problems of CuO can be solved [41, 46, 47]. For example, neither sintering nor agglomeration was demonstrated for CuO supported on Al_2O_3 prepared by co-precipitation [34]. However, during this study particle attrition was observed after 7 cycles of combustion over CuO/Al_2O_3 as seen from both the SEM images and sieving measurements, with approximately 77 wt. % of the particles reduced in size from 53-150 μm to less than 53 μm (Table 3). Further details about the surface of both fresh and used oxygen carriers presented in Fig. B2 in Appendix B as SEM images.

3.7. Possible reaction pathways, kinetic analysis and potential applications

For CLC to be selective for n-heptane and n-hexadecane, this strongly suggested that the reactions initiated by bond cleavage are either thermolytic, leading to radicals, or catalytic, leading to carbocations. The sharp cut-off in combustion efficiency as the temperature falls below 380 °C probably represents the point where the extent of bond cleavage falling to a negligible level.

Virtually complete CLC has been achieved with no evidence of coke formation. As suggested by Hoteit et al. [13], a large proportion of the fuels appeared to have oxidised almost immediately at injection, with the low CO/CO_2 ratios demonstrating that the partial combustion of both n-hexadecane and n-heptane is negligible. Moreover, Moldenhauer et al. [25] observed that once the temperature falls below 950 °C, the reaction from the fuel to form $CO+H_2$ is slower than that of $CO+H_2$ to CO_2+H_2O. Additionally, no coke deposition was observed on the oxygen carriers CuO and Mn_2O_3, consistent with studies at higher temperatures [41, 45].

Depending upon the feed flow rate, the liquid fuels may enter the oxygen carrier bed in the form of both droplets and in the vapour phase. The former would be expected to be more prevalent for n-hexadecane due to its higher boiling point, but the results in Fig.4 suggest that n-hexadecane passed through the oxygen carrier bed in the form of vapour.

To carry out kinetic analysis for n-hexadecane CLC with CuO, it was assumed that the liquid fuel entered the reactor in the form of droplets and went through the oxygen carrier bed in the vapour phase with the carrier gas, N_2. The order of the reaction (n) (Fig. C2.a) of 1.6 was determined using the steady state material balance for plug flow reactor (Fig. C1) for four different volumetric feed flow rates; 0.03, 0.1, 0.2, and 1.4 ml/min, at 482 °C. The activation energy (E) of 24.5 kJ/mol was calculated using an Arrhenius plot (Fig. C2.b) for n-hexadecane with CuO. A wide range of activation

energies have been reported [48-50], 60, 33 and 14 kJ/mol for CLC of methane, hydrogen, and CO, respectively, with different oxygen carriers. Obviously, the activation energies for the combustion of methane, hydrogen, and CO cannot strictly be compared with those for the combustion of higher hydrocarbons. However, due to the lack of information for liquid fuel combustion with oxygen carriers, no comparisons can be made for preliminary empirical kinetic findings presented here.

The reported findings suggest that CLC can potentially be used for hot gas clean-up, either to remove unburnt hydrocarbons and potentially other volatile organic species from flue gases or hot methane streams. Clearly, aromatic hydrocarbons and other compounds need to be tested to define the potential scope for these applications. The lighter n-alkanes, ethane, propane and butane, are expected to react slower than n-heptane and n-hexadecane due to their much stronger C-C bonds, as shown by the decrease in the cracking activity of alkanes with a decrease in their carbon number [51]. Similarly, low temperature CLC may not be applicable for the combustion of the polycyclic aromatic hydrocarbons to the strong aromatic C-C bonds.

4. Conclusions

This study has established that selective CLC of higher alkanes over methane can be achieved with CuO and Mn_2O_3, at temperatures below 500 °C. Under fuel-lean ($0<\phi<1$) conditions, it is possible to achieve high levels of combustion of n-heptane and n-hexadecane over CuO at ϕ: 0.7. Additionally, in fuel-rich conditions ($1<\phi<\infty$), it is also possible to reach the maximum extent of combustion of n-hexadecane and n-heptane with CuO with ϕ >1.3 at 482 °C with a residence time of 13 s. CuO can be fully reduced to Cu in low temperature CLC. However, the combustion efficiency for Mn_2O_3 was limited by the slow second reduction step (Mn_3O_4 to MnO). Sintering of CuO in a multi-cycle test was observed, but this can be avoided by using an Al_2O_3 support. Kinetic analysis for the combustion of n-hexadecane indicated a reaction order of 1.6 and a relatively high activation energy of 24.5 kJ/mol. The high selectivity achieved for higher hydrocarbons suggests the low temperature CLC can be used for hot gas clean-up to remove higher alkanes and potentially other volatile organic compounds.

To develop further this concept, other higher hydrocarbons than alkanes need to be tested, for example alkenes and aromatics need to be tested in order to define the potential scope of the application of low temperature CLC. Additionally, while it is observed that using supported oxygen carriers eliminated sintering and agglomeration over a few cycles, this needs to be investigated in greater detail.

Acknowledgment

The authors thank the Nanoscale and Microscale Research Centre (nmRC) for providing access to SEM instrumentation.

References

[1] Ksepko E, Siriwardane RV, Tian H, Simonyi T, Sciazko M. Effect of H_2S on chemical looping combustion of coal-derived synthesis gas over Fe–Mn oxides supported on sepiolite, ZrO_2, and Al_2O_3. Energy & Fuels 2012;26(4):2461-72.

[2] Rydén M. Chemical looping combustion of liquid fuels. In: Fennell P, Anthony B, editors. Calcium and chemical looping technology for power generation and carbon dioxide (CO_2) capture. Elsevier; 2015, p. 287-98.

[3] Han L, Bollas GM. Dynamic optimization of fixed bed chemical-looping combustion processes. Energy 2016;112:1107-19.

[4] Zhu L, He Y, Li L, Wu P. Tech-economic assessment of second-generation CCS: Chemical looping combustion. Energy 2018;144:915-27.

[5] Han L, Bollas GM. Chemical-looping combustion in a reverse-flow fixed bed reactor. Energy 2016;102:669-81.

[6] Khakpoor N, Mostafavi E, Mahinpey N, De la Hoz Siegler H. Oxygen transport capacity and kinetic study of ilmenite ores for methane chemical-looping combustion. Energy 2018.

[7] Kerr HR. Capture and seperation technology gaps and priority research needs. In: Thomas DC, ed. Carbon dioxide capture for storage in deep geologic formations – Results from the CO_2 capture project. 1. Elsevier; 2005:655-60.

[8] Rubin ES, Mantripragada H, Marks A, Versteeg P, Kitchin J. The outlook for improved carbon capture technology. Progress in Energy and Combustion Science 2012;38(5):630-71.

[9] Lockwood T. A compararitive review of next-generation carbon capture technologies for coal-fired power plant. Energy Procedia 2017;114:2658-70.

[10] García-Labiano F, de Diego LF, García-Díez E, Serrano A, Abad A, Gayán P, et al. Combustion and reforming of liquid fossil fuels through chemical looping processes: Integration of chemical looping processes in a refinery. Energy Procedia 2017;114:325-33.

[11] Álvaro ÁJ, Montesino ÁU, Orgaz SS, Fernández CG. Thermodynamic analysis of a dual power-hydrogen production system based on chemical-looping combustion. Energy 2017;137:1075-85.

[12] Mishra N, Bhui B, Vairakannu P. Comparative evaluation of performance of high and low ash coal fuelled chemical looping combustion integrated combined cycle power generating systems. Energy 2018.

[13] Hoteit A, Forret A, Pelletant W, Roesler J, Gauthier T. Chemical looping combustion with different types of liquid fuels. Oil & Gas Science and Technology 2011;66(2):193-9.

[14] Zhang X, Han W, Hong H, Jin H. A chemical intercooling gas turbine cycle with chemical-looping combustion. Energy 2009;34(12):2131-6.

[15] Frick V, Rydén M, Leion H, Mattisson T, Lyngfelt A. Screening of supported and unsupported Mn–Si oxygen carriers for CLOU (chemical-looping with oxygen uncoupling). Energy 2015;93:544-54.

[16] Lyngfelt A. Chemical-looping combustion of solid fuels–status of development. Applied Energy 2014;113:1869-73.

[17] Mattisson T, Lyngfelt A, Leion H. Chemical-looping with oxygen uncoupling for combustion of solid fuels. International Journal of Greenhouse Gas Control 2009;3(1):11-9.

[18] Adanez J. Chemical looping combustion of gaseous fuels. In: Fennell P, Anthony B, editors. Calcium and chemical looping technology for power generation and carbon dioxide (CO_2) capture. Elsevier; 2015, p. 256-85.

[19] Adanez J, Abad A, Garcia-Labiano F, Gayan P, de Diego LF. Progress in chemical-looping combustion and reforming technologies. Progress in Energy and Combustion Science 2012;38(2):215-82.

[20] Cao Y, Li B, Zhao H-Y, Lin C-W, Sit SP, Pan W-P. Investigation of asphalt (bitumen)-fuelled chemical looping combustion using durable copper-based oxygen carrier. Energy Procedia 2011;4:457-64.

[21] Bao J, Liu W, Cleeton JPE, Scott SA, Dennis JS, Li Z, et al. Interaction between Fe-based oxygen carriers and n-heptane during chemical looping combustion. Proceedings of the Combustion Institute 2013;34(2):2839-46.

[22] Serrano A, García-Labiano F, de Diego LF, Gayán P, Abad A, Adánez J. Chemical looping combustion of liquid fossil fuels in a 1 kW th unit using a Fe-based oxygen carrier. Fuel Processing Technology 2017;160:47-54.

[23] Moldenhauer P, Rydén M, Mattisson T, Lyngfelt A. Chemical-looping combustion and chemical-looping with oxygen uncoupling of kerosene with Mn- and Cu-based oxygen carriers in a circulating fluidized-bed 300W laboratory reactor. Fuel Processing Technology 2012;104:378-89.

[24] Moldenhauer P, Rydén M, Mattisson T, Lyngfelt A. Chemical-looping combustion and chemical-looping reforming of kerosene in a circulating fluidized-bed 300W laboratory reactor. International Journal of Greenhouse Gas Control 2012;9:1-9.

[25] Moldenhauer P, Rydén M, Mattisson T, Hoteit A, Jamal A, Lyngfelt A. Chemical-looping combustion with fuel oil in a 10 kW pilot plant. Energy & Fuels 2014;28(9):5978-87.

[26] Moldenhauer P, Rydén M, Mattisson T, Younes M, Lyngfelt A. The use of ilmenite as oxygen carrier with kerosene in a 300W CLC laboratory reactor with continuous circulation. Applied Energy 2014;113:1846-54.

[27] Moldenhauer P, Rydén M, Mattisson T, Jamal A, Lyngfelt A. Chemical-looping combustion with heavy liquid fuels in a 10 kW pilot plant. Fuel Processing Technology 2017;156:124-37.

[28] Spinelli M, Peltola P, Bischi A, Ritvanen J, Hyppänen T, Romano MC. Process integration of chemical looping combustion with oxygen uncoupling in a coal-fired power plant. Energy 2016;103:646-59.

[29] Siriwardane R, Tian H, Miller D, Richards G, Simonyi T, Poston J. Evaluation of reaction mechanism of coal–metal oxide interactions in chemical-looping combustion. Combustion and flame 2010;157(11):2198-208.

[30] Xu L, Li Z, Sun H, Bao J, Cai N. Low-temperature chemical looping combustion for removing unburnt gaseous components with a cement-supported CuO oxygen carrier. Energy & Fuels 2013;27(11):6872-9.

[31] Medrano JA, Hamers H, Williams G, van Sint Annaland M, Gallucci F. $NiO/CaAl_2O_4$ as active oxygen carrier for low temperature chemical looping applications. Applied Energy 2015;158:86-96.

[32] van Straelen J, Geuzebroek F, Goodchild N, Protopapas G, Mahony L. CO_2 capture for refineries, a practical approach. International Journal of Greenhouse Gas Control 2010;4(2):316-20.

[33] International ASTM. Standard Test Method for Testing Fluid Catalytic Cracking (FCC) Catalysts by Microactivity Test. ASTM International ASTM D3907-13; 2013:1-6.

[34] Chuang S, Dennis J, Hayhurst A, Scott S. Development and performance of Cu-based oxygen carriers for chemical-looping combustion. Combustion and Flame 2008;154(1-2):109-21.

[35] Chuang S, Dennis J, Hayhurst A, Scott S. Kinetics of the chemical looping oxidation of CO by a co-precipitated mixture of CuO and Al_2O_3. Proceedings of the Combustion Institute 2009;32(2):2633-40.

[36] Chuang S, Dennis J, Hayhurst A, Scott S. Kinetics of the chemical looping oxidation of H2 by a co-precipitated mixture of CuO and Al_2O_3. Chemical Engineering Research and Design 2011;89(9):1511-23.

[37] Jin H, Ishida M. Reactivity study on natural-gas-fueled chemical-looping combustion by a fixed-bed reactor. Industrial & engineering chemistry research 2002;41(16):4004-7.

[38] Corbella BM, De Diego L, García F, Adánez J, Palacios JM. The performance in a fixed bed reactor of copper-based oxides on titania as oxygen carriers for chemical looping combustion of methane. Energy & Fuels 2005;19(2):433-41.

[39] Flagan RC, Seinfeld JH. Fundamentals of air pollution engineering. Mineola New York: Courier Corporation; 2012.

[40] Law CK. Combustion physics. Cambridge University Press; 2010.

[41] Adánez J, Gayán P, Celaya J, de Diego LF, García-Labiano F, Abad A. Chemical looping combustion in a 10 kWth prototype using a CuO/Al2O3 oxygen carrier: Effect of operating conditions on methane combustion. Industrial & engineering chemistry research 2006;45(17):6075-80.

[42] Luis F, Garcı F, Gayán P, Celaya J, Palacios JM, Adánez J. Operation of a 10kWth chemical-looping combustor during 200h with a $CuO–Al_2O_3$ oxygen carrier. Fuel 2007;86(7):1036-45.

[43] Forero C, Gayán P, García-Labiano F, De Diego L, Abad A, Adánez J. High temperature behaviour of a $CuO/\gamma Al_2O_3$ oxygen carrier for chemical-looping combustion. International Journal of Greenhouse Gas Control 2011;5(4):659-67.

[44] Gayán P, Forero CR, Abad A, de Diego LF, García-Labiano F, Adánez J. Effect of support on the behavior of Cu-based oxygen carriers during long-term CLC operation at temperatures above 1073 K. Energy & Fuels 2011;25(3):1316-26.

[45] Cao Y, Casenas B, Pan W-P. Investigation of chemical looping combustion by solid fuels. 2. Redox reaction kinetics and product characterization with coal, biomass, and solid waste as solid fuels and CuO as an oxygen carrier. Energy & Fuels 2006;20(5):1845-54.

[46] De Diego LF, Gayán P, García-Labiano F, Celaya J, Abad A, Adánez J. Impregnated CuO/Al_2O_3 oxygen carriers for chemical-looping combustion: avoiding fluidized bed agglomeration. Energy & Fuels 2005;19(5):1850-6.

[47] Siriwardane R, Tian H, Richards G, Simonyi T, Poston J. Chemical-looping combustion of coal with metal oxide oxygen carriers. Energy & Fuels 2009;23(8):3885-92.

[48] García-Labiano F, de Diego LF, Adánez J, Abad A, Gayán P. Reduction and oxidation kinetics of a copper-based oxygen carrier prepared by impregnation for chemical-looping combustion. Industrial & engineering chemistry research 2004;43(26):8168-77.

[49] Garcia-Labiano F, Adánez J, de Diego LF, Gayán P, Abad A. Effect of pressure on the behavior of copper-, iron-, and nickel-based oxygen carriers for chemical-looping combustion. Energy & Fuels 2006;20(1):26-33.

[50] Abad A, García-Labiano F, de Diego LF, Gayán P, Adánez J. Reduction kinetics of Cu-, Ni-, and Fe-based oxygen carriers using syngas ($CO+ H_2$) for chemical-looping combustion. Energy & Fuels 2007;21(4):1843-53.

[51] Kissin YV. Chemical mechanisms of catalytic cracking over solid acidic catalysts: alkanes and alkenes. catalysis reviews 2001;43(1-2):85-146.

Highlights:

- CLC of nC_7 and nC_{16} with CuO and Mn_2O_3 as oxygen carriers at 482 °C achieved
- Very high levels of combustion over CuO in fuel-lean (ϕ<0.7) conditions at 482°C
- Low Temperature CLC is selective for higher hydrocarbons, methane does not react
- Such selectivity suggests reaction with oxygen involves radicals from bond scission